

# Experimental observation of direct bandgap photoluminescence from tensile-strained Ge nanodots embedded within SiO<sub>2</sub> matrix

M. H. Kuo<sup>1</sup>, S. K. Chou<sup>1</sup>, W. T. Lai<sup>2</sup>, Y. W. Pan<sup>2</sup>, S. D. Lin<sup>2</sup>, Tom George<sup>2</sup>, and P. W. Li<sup>1,2</sup>

<sup>1</sup> Department of Electrical Engineering, National Central University, Jongli, Taoyuan, Taiwan, 320

<sup>2</sup> Department of Electronics Engineering, National Chiao Tung University, Hsinchu, Taiwan, 30010

## Abstract

**Microdisk-arrays of vertically-stacked Ge nanodots of 30–70nm in diameter embedded within SiO<sub>2</sub> layers were fabricated using thermal oxidation of Si<sub>0.75</sub>Ge<sub>0.25</sub> abacus-shaped nano-pillars and followed by thermal annealing in oxygen-deficient conditions. The Ge nanodots are subjected to increasing tensile-strain by reducing dot size. As much as 3.2% tensile strain can be generated within 30nm Ge nanodots embedded within SiO<sub>2</sub>, facilitating direct-bandgap photoluminescence from Ge nanodots. Temperature-insensitive carrier lifetimes of 2.8 and 5ns for the HH and LH valence band transitions, respectively, are also measured at 10–100 K.**

## 1. Introduction

Ge-on-Si appears to be the most promising candidate for active photonic devices such as photodetectors, modulators, and light emitters thanks to its pseudo-direct gap behavior, high absorption coefficient, and process compatibility with prevailing Si electronics. The key for efficient light emission from or absorption by Ge lies in boosting direct band-to-band transition, which is challenging because Ge is generally recognized as an indirect-gap material. Fortunately, direct-bandgap Ge is feasible by taking advantage of a small energy difference (0.14eV) between its L— $\Gamma$  valleys. Significant efforts are being made to enhance direct bandgap transition in Ge by virtue of high concentration *n*-doping and tensile-strain engineering. However, the efficiency of experimentally-demonstrated, optical-pumping Ge laser using tensile-strain (>1.7%) and *n*-doping (>10<sup>19</sup>cm<sup>-3</sup>) engineering is yet of satisfactory [1], possibly due to free-carrier absorption. Aside from strained thin-films Ge, Ge nanostructures are also promising to achieve direct light emission [2]. In this paper, we report experimental observation of direct gap photoluminescence (PL) from tensile-strained 32.4±7.8nm Ge nanodots embedded within thermally-growing SiO<sub>2</sub> matrix.

## 2. Experimental results and discussion

Process flow and the corresponding SEM/TEM/EDX micrograph of Ge-nanodot microdisk array is summarized in Fig. 1. Good crystallinity of the Ge nanodots is evidenced by the clear lattice fringes and sharp diffraction spots from high-resolution transmission electron microscopy (HRTEM) and selected-area diffraction (SAD) observations. A considerable redshift of 12.88 cm<sup>-1</sup> for the longitudinal optical (LO) Ge-Ge phonon mode was measured on the 32.4±7.8 nm Ge nanodots compared to the bulk Raman line of 301.5 cm<sup>-1</sup> (Fig. 2). The estimated tensile strain for the 32.4±7.8nm Ge dots is 3.2%. Another important finding is the absence of the GeO<sub>2</sub>

signal in the spectral shift of 440cm<sup>-1</sup>, indicating the chemical purity of the Ge nanodots embedded within SiO<sub>2</sub> layers.

Further strong support for large tensile strains in our Ge nanodots embedded within SiO<sub>2</sub> layers is the observation of strain-split direct bandgap transitions to the light-hole (LH) and heavy-hole (HH) VBs at energies of 0.82–0.85eV and 0.86–0.9eV, respectively, from temperature- and power-dependent PL measurements. Figure 3 shows PL spectra measured on Ge nanodots at temperatures of 10–200K. A main PL peak centered at 0.85eV together with a satellite peak at 0.90eV is attributable to the direct bandgap transitions from the  $\Gamma_{CB}$  valley to the LH ( $\Gamma_{CB}-\Gamma_{LH}$ ) and to the HH ( $\Gamma_{CB}-\Gamma_{HH}$ ), respectively. A blue shift for PL energy ( $E_D$ ) is observed when decreasing temperature and could be fitted by using Varshni's type equation in terms of  $E_D(T)=E_{D0}-\alpha T^2/(T+\beta)$ , where  $E_{D0, \Gamma-LH} = 0.845$  eV,  $\alpha_{\Gamma-LH} = 3.2 \times 10^{-4}$  eV/K and  $\beta_{\Gamma-LH} = 301.7$  K as well as  $E_{D0, \Gamma-HH} = 0.897$  eV,  $\alpha_{\Gamma-HH} = 5.7 \times 10^{-4}$  eV/K and  $\beta_{\Gamma-HH} = 426.8$  K for  $\Gamma_{CB}-\Gamma_{LH}$  and  $\Gamma_{CB}-\Gamma_{HH}$  transitions. The PL energy of 32.4±7.8 nm Ge QDs at 10 K is nearly invariant with excitation power ranging from 4–13.4mW (Fig. 4), whereas a monotonic increase in PL integrated intensity at 0.85 eV and 0.9 eV is induced by increasing the excitation power in a linear relationship of  $I_{PL} \propto P^{0.99}$  and  $I_{PL} \propto P^{1.05}$ , respectively. Once again, the power dependency of PL intensity suggests PL emission being predominated by the direct exciton recombination in Ge QDs.

Fig. 5 shows the temperature evolution of transient direct bandgap PL curves for the Ge nanodots from 10K to 100K. The detection energies were fixed at the PL peak energy of 0.9–0.82eV for different temperatures. The extracted decay times of  $\tau_{\Gamma-LH} = 4.9-5.1$ ns and  $\tau_{\Gamma-HH} = 2.7-2.85$ ns remain nearly unchanged with temperature and are much less than the bulk values of Ge. Once again, the temperature-insensitive decay time for both  $\Gamma$ -HH and  $\Gamma$ -LH transitions agrees with the observed PL at 0.9eV and 0.85eV originating from exciton radiative recombination.

## 3. Conclusion

We report the fabrication of vertically-stacked Ge nanodots embedded within SiO<sub>2</sub> through thermal oxidation of SiGe nanopillars followed by post-annealing in an oxygen deficient conditions. Large (as much as 3.2%) tensile strains can be generated in the Ge nanodots by the local embedded layers of SiO<sub>2</sub>, indeed facilitating the direct bandgap PL from the Ge nanodots and the strain-split direct-bandgap transitions to the LH and HH bands. Between 10–100 K temperature-insensitive carrier lifetimes of 2.7ns and 5ns were measured for the transitions to HH and LH bands, respectively, in the Ge nanodots, thanks to our enhanced oscillator strength.

#### 4. References

- [1] J. Liu et al., Optics Express, 15, 11272, 2007.  
 [2] S Manna et al., J. Phys. D: Appl. Phys. 48, 215103, 2015.

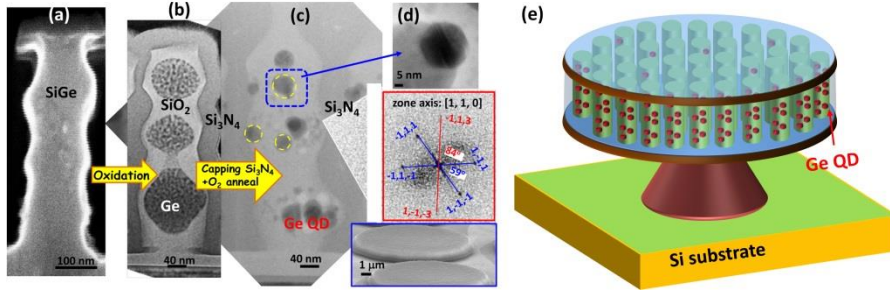


Fig. 1 (a-c) Schematic diagram, and CTEM micrograph of the experimental Ge-QD microdisk, (d) HRTEM of a single Ge nanodot and corresponding SAD patterns showing the high degree of crystallinity within the Ge nanodots, and (e) fabrication schematics of the ultimate microdisk arrays of Ge nanodots.

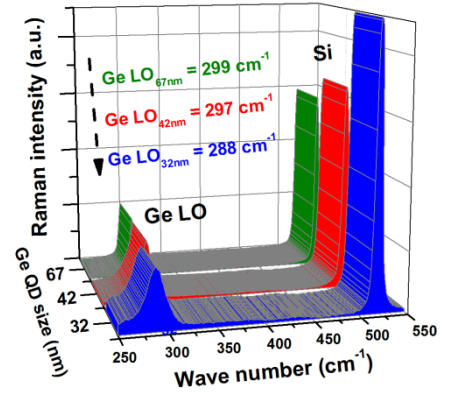


Fig. 2. Raman spectra of the Ge QD embedded in SiO<sub>2</sub>.

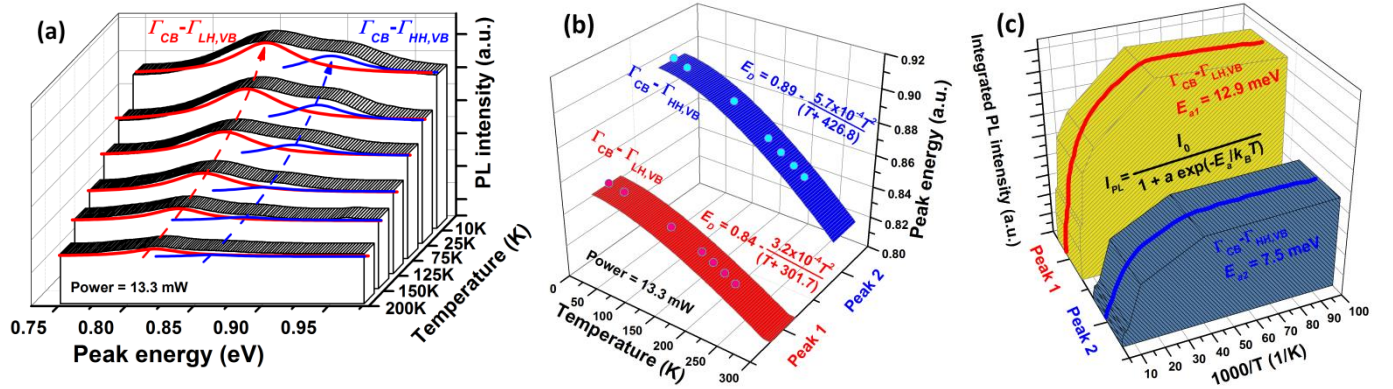


Fig. 3 (a) Temperature-dependent PL spectra of Ge QDs and PL peak energy plotted as a function of temperature from 20 to 200 K. (b) Direct bandgap related PL peak energies ( $E_D$ ) plotted as a function of temperature from 10 to 200 K. (c) Arrhenius plot of integrated PL intensity as a function of temperature for the 32.4±7.8 nm Ge dots.

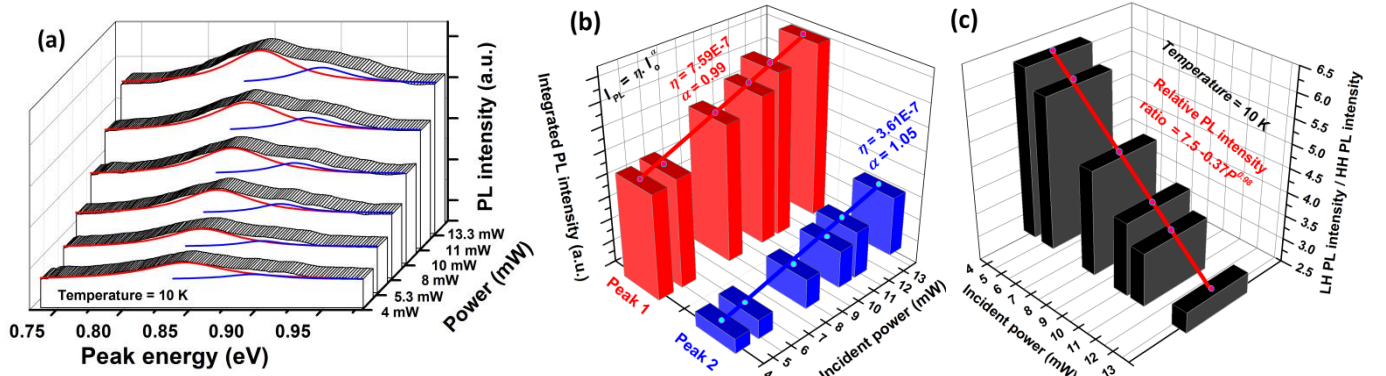


Fig. 4 (a) Power-dependent PL spectra and integrated PL intensity of Ge QDs measured at 10 K. (b) The integral PL intensity of both P1 and P2 peaks appears to have a linear dependence on the excitation laser power in a form of  $I_{PL} \propto I_0$ , and (c) Relative intensity of  $I_{P1}/I_{P2}$  declines with increasing excitation power.

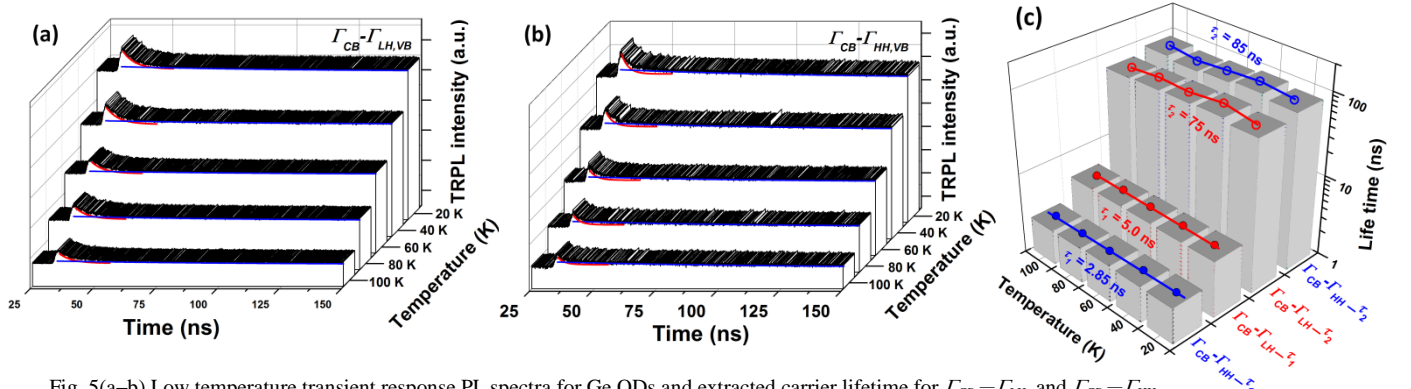


Fig. 5(a-b) Low temperature transient response PL spectra for Ge QDs and extracted carrier lifetime for  $\Gamma_{CB} - \Gamma_{LH}$  and  $\Gamma_{CB} - \Gamma_{HH}$ . (c) extracted carrier lifetime for  $\Gamma_{CB} - \Gamma_{LH,VB}$  and  $\Gamma_{CB} - \Gamma_{HH,VB}$  is nearly constant at temperatures of 10–100K.